Acta Cryst. (1995). B51, 255–260

X-ray Diffraction and Computer Modelling Study of the Structure and Conformation of Poly(3-decylthiophene)

BY W. ŁUŻNY

Faculty of Physics and Nuclear Techniques, University of Mining and Metallurgy, Al. Mickiewicza 30, 30-059 *Cracow, Poland*

(*Received* 13 *January* 1994; *accepted* 15 *September* 1994)

Abstract

The results of the computer modelling for the conformation of poly(3-decylthiophene) are presented and compared with experimental X-ray diffraction data. Since the conformation of the polymer chain is correlated with the relative intensity of Bragg reflections of the proposed structure, modelling-supported X-ray diffraction analysis allows information concerning the structure of the polymer to be obtained. The best agreement of the model diffraction pattern with the experimental data could be obtained for two structures. For one, the torsion angle α in the dimer is 30° and the torsion angle β between two dimers is 65°, and for the other, $\alpha \cong 65$ and $\beta \cong 30°$.

Introduction

X-ray diffraction still remains the main method for structural investigations of polymers. Because of the complexity of the polymer structures, the interpretation of the diffraction data may be difficult. The common methods of structure determination (*e.g.* the Rietveld method) sometimes cannot give reasonable results since only a few crystalline peaks are usually present in experimental diffractograms and the unit cell of a typical polymer may contain several dozens of atoms. Besides, it may be difficult to distinguish between peaks of the crystalline origin and peaks of the amorphous origin. In such cases computer modelling can be of help in the elucidation of the structure of polymers.

This approach, involving computer modelling to best reproduce the experimentally observed Bragg reflections, has been used in studies on poly(3-decylthiophene) (PDT).

The crystalline structure of PDT has been investigated by several authors (Gustaffson, Inganäs, Österholm & Laakso, 1991; Mårdalen, Samuelsen, Gautun & Carlsen, 1992; Winokur, Wamsley, Moulton, Smith & Heeger, 1991; Hsu, Levon, Ho, Myerson & Kwei, 1993; Tashiro, Minagawa, Kobayashi, Morita & Yoshino, 1993). Our results (Łużny, Nizioł, Zagórska & Proń, 1993; Łużny, Nizioł & Proń, 1995; Łużny, Nizioł, Straczyński & Proń, 1994) are in good agreement with these literature data. Thus, the main goal of this work was to show how (by the use of computer modelling) to obtain accurate information concerning the molecular conformation of the polymer.

The model of the crystalline structure of PDT

The monomer of PDT, 3-decylthiophene ($C_{14}H_{22}S_1$) consists of a thiophene ring with a decyl group substituted at C3. The structure of this compound, with the covalent bond parameters, is presented in Fig. 1. These parameters, taken from Visser, Heeres, Wolters & Vos (1968) have been used to calculate the coordinates of the atoms in the modelled structures.

The crystalline structure of PDT can be explained with an orthorhombic unit cell; the experimental diffractogram is typical of a layered structure with the main chains stacked on top of each other, forming parallel planes separated by the decyl side chains. The unit cell assumed in this work is presented in Fig. 2. The starting point of the modelling was the flat system of four thiophene rings with four decyl groups.

The lattice constants ($a = 23.9$, $b = 15.6$ and $c = 3.8$ Å) have been fitted to the experimental diffractogram, presented in Fig. 3.

The experimental diffraction data for PDT

The X-ray diffractograms were obtained in the reflection mode using a HZG-4 wide-angle diffractometer. A Cu anode tube with a Ni filter and a crystalline mono-

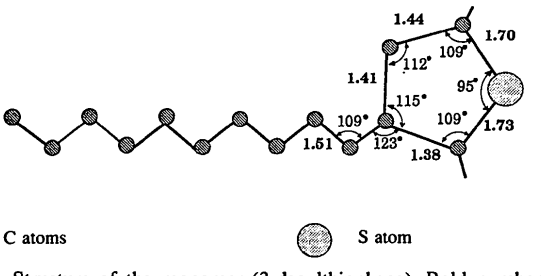

Fig. 1. Structure of the monomer (3-decylthiophene). Bold numbers represent the lengths of the covalent bonds (Å). All H atoms have been omitted for clarity.

chromator behind the sample were used. The sample (thin film with thickness 30–60 μm) was not oriented prior to the measurement, and was placed in the home-made apparatus for the stretching of samples; construction of this device avoids the background from the sample holder. The data were recorded on computer.

The experimental diffraction pattern presented in Fig. 3 was fitted with a set of Gaussian or Lorentzian peaks located on a flat linear background. The characteristics of these peaks are collected in Table 1. It is obvious that the quality of this diffractogram is very low: the background is high, the amorphous component of scattered intensity is very large, there are only a few peaks and (excluding the first) they have a very low relative intensity and large width. Without additional information, it is virtually impossible (except for peak no. 1 of crystalline origin and peak no. 5 of amorphous origin) to distinguish between the peaks of the crystalline origin and those of amorphous origin.

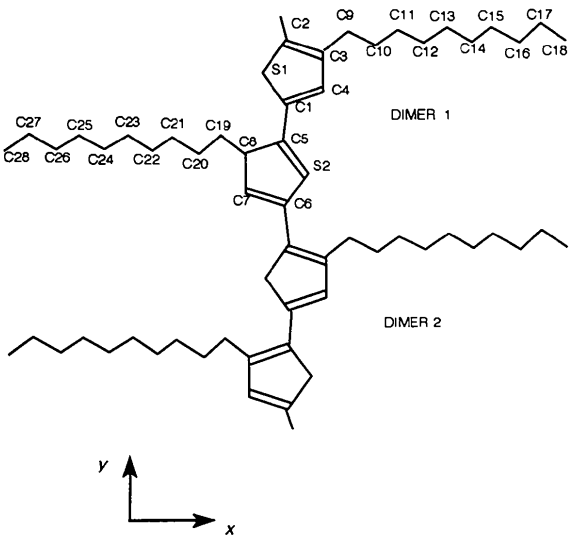

Fig. 2. Scheme of the model structure of PDT within one unit cell.

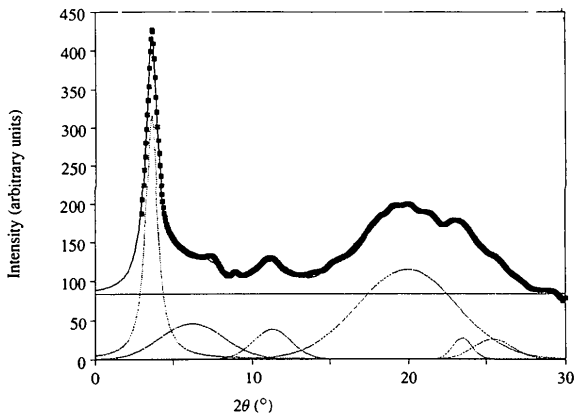

Fig. 3. X-ray diffraction pattern of PDT. The experimental data are approximated by a linear background and a set of Gaussian or Lorentzian functions.

Table 1. *Parameters of analytical functions fitted to the experimental data (L = Lorentzian, G = Gaussian)*

No	Type	Amplitude (arbitrary units)	Position, 2θ (°)	Width (°)
1	L	315.9	3.65	0.89
2	G	45.2	6.18	4.68
3	G	3.8	8.98	0.27
4	G	37.4	11.28	2.84
5	G	114.5	19.94	7.39
6	G	26.3	23.48	1.47
7	G	24.7	25.41	2.88

The large width of the Bragg peaks is associated with the small size of the crystalline regions in the polymer. Usually the diameter of such crystalline lamellae does not exceed 100–200 Å; in the case of PDT it can be even lower (particularly in the direction perpendicular to the main chains of the polymer), which was confirmed by our SAXS observations (Łużny, Ślusarczyk & Włochowicz, 1991).

The results of the fitting procedure applied to the PDT diffraction data should be considered only as an approximation and the parameters of fitted functions, collected in Table 1, must be treated as a crude estimation of the real situation.

Modelling of structure and conformation

The computation of the intensity of Bragg peaks for the assumed crystalline structure first requires the determination of the positions of all atoms in the unit cell. We started with the basic model of the structure, described above and presented in Figs. 1 and 2. The most important conformational defects in PDT are connected with the non-planarity of the main polymer chains. Such an effect was described for poly(3-hexylthiophene) (Salaneck, Inganäs, Thémans, Nilsson, Sjögren, Österholm, Brèdas & Svensson, 1988; Salaneck, 1989) as an explanation of the thermochromism phenomena; the scheme of such an effect is shown in Fig. 4. Therefore, we have tried to consider here the possibility of twisting one thiophene ring around the bond with the adjacent thiophene ring.

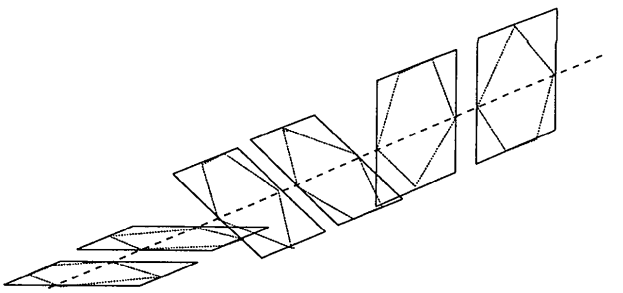

Fig. 4. Scheme of the relative orientation of several thiophene rings in a polymer chain, proposed by Salaneck (1989).

The procedure of modelling involves the following steps (also schematically sketched in Fig. 5):

(*a*) we start with the flat system of the two thiophene rings with two alkyl groups [Fig. 5(*a*)];

(*b*) one monomer is twisted around the C1—C5 bond with an assumed angle α [Fig. 5(*b*)];

(*c*) the dimer or the system of both monomers is duplicated [Fig. 5(*c*)];

(*d*) the second dimer is twisted with an assumed angle β [Fig. 5(*d*)];

(*e*) finally, the whole system of four monomers (or two dimers) is twisted around an axis of the chain such that the axis of symmetry of a projection of the system is perpendicular to the original plane of the system [Fig. 5(*e*)].

The last step of the procedure described above is a simple consequence of the necessity of minimalization of the average deflection of monomers from their original plane; this condition is related to the problem of arrangement of the adjacent polymer chain (upper and lower).

One can see that our model of PDT conformation has two free parameters, α and β. The relation between these parameters and the intensity of diffraction peaks is explained below.

Calculations of diffraction patterns

The intensity of Bragg peaks (for X-ray powder diffraction) can be explained by the following formula

$$I = I_o N^2 F^2 LPMD,$$

where I_o is the intensity of a primary beam, N the number of unit cells, F the structure factor, L the Lorentz factor, P the polarization factor, M the multiplication factor for crystal planes, and D the Debye–Waller factor.

In model calculations, only the relative intensities of the diffraction peaks are computed. In the modelling presented below the intensity of the highest maximum is identical in all the diffractograms obtained.

There are two reasons for the broadening of the peaks: sample factors and apparatus factors. The sample factors are mainly connected to the sizes of the crystalline regions (as discussed above). It is difficult to consider them in the modelling procedure, because the well known Debye–Scherrer formula giving the relation between the width of Bragg peak and the size of a crystallite is not well applicable to paracrystalline materials such as polymers. The apparatus factors (problems of monochromatization and collimation mainly) can be described analytically and have been considered in our calculations.

Finally, our model diffraction patterns do not have any background or amorphous component of scattered intensity. Comparison with the experimental diffraction patterns is therefore possible only by comparing the position of peaks, and their relative heights.

Results of computer modelling

The diffraction pattern of the initial flat system (Fig. 1) should be taken as a starting point of the modelling procedure. Such a structure is described by $\alpha = \beta = 0$. The resulting diffraction pattern is presented in Fig. 6. It can be considered only as an extremely crude approximation to the real diffractogram. The positions of the peaks (especially the first one) are almost correct, but their relative intensities are very different from the experimentally determined ones. The model diffractogram can be characterized by a set of three parameters, giving the ratios of intensities of three consecutive peaks

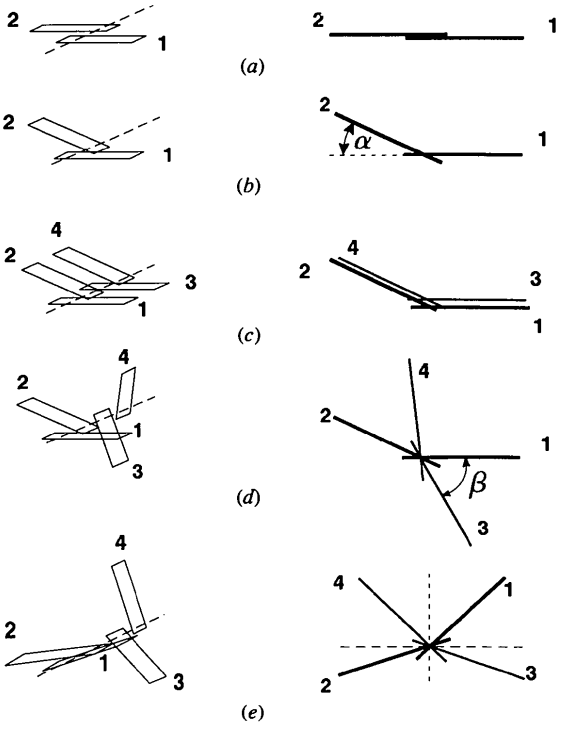

Fig. 5. The five-steps procedure of the conformation modelling.

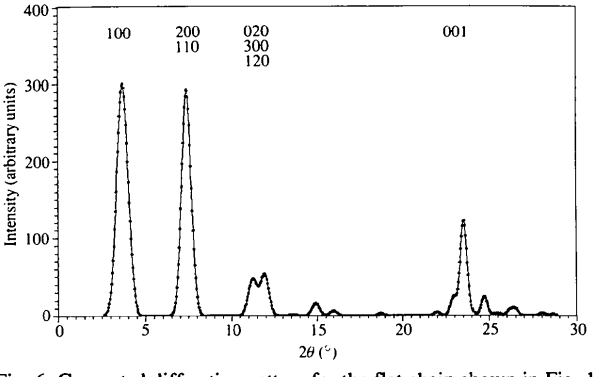

Fig. 6. Computed diffraction pattern for the flat chain shown in Fig. 1.

to the intensity of the first one. We thus have

$$N_{2/1} = I(110, 200)/I(100) \times 100\%,$$
$$N_{3/1} = I(300, 020, 120)/I(100) \times 100\%, \text{ and}$$
$$N_{4/1} = I(001)/I(100) \times 100\%.$$

The parameter $N_{4/1}$ is very sensitive to the increase in α and β angles, and it quickly approaches zero. Therefore, in further analyses we will concentrate on the two former parameters. Their experimental values, estimated from the data collected in Table 1, are as follows: $N_{2/1} \cong 14\%$ and $N_{3/1} \cong 12\%$. The best method of finding the values of α and β for which $N_{2/1}$ and $N_{3/1}$ would be close to their experimental approximations is to compute the diffraction patterns for the model structures with the parameters α and β varying in a wide range. The results of such computations are presented as maps in Figs. 7 and 8. The parameters $N_{2/1}$ and $N_{3/1}$ have the correct values along two contour lines. Because we need the coincidence of the two events, we have collected the contour lines from both maps in the interesting ranges $13.5 < N_{2/1} < 14.5\%$ and $11.5 < N_{3/1} < 12.5\%$, in one map, as shown in Fig. 9. $N_{2/1}$ and $N_{3/1}$ have values close to their experimental estimation, since the angles α and β concentrate into two regions, where two groups of contour lines cross. These areas, marked in Fig. 9, are at $\alpha \cong 30°$, $\beta \cong 65°$ (for the first area), and $\alpha \cong 65°$, $\beta \cong 30°$ (for the second area). The diffraction patterns computed for these two sets of parameters α and β are identical and such a diffractogram is presented in Fig. 10.

If the analogous computations are carried out with the omission of the last step of the procedure described above [Fig. 5(*e*)], no crossing exists between the contour lines and α and β do not reproduce the real diffractogram.

The coordinates of the atoms in the unit cell, used for the structure-factor calculations (for the two best models of conformation), have been deposited.* These two best model structures are shown in Fig. 11.

Discussion and conclusions

There is a striking symmetry between the values of α and β, for which the N parameters fall into the expected ranges. Of course, this symmetry arises from the general symmetry properties of the maps presented in Figs. 7 and 8. For the procedure of conformation modelling described above, we obtain the final arrangement of the planes of monomers, which can be characterized by a set of four angles between the actual plane of the monomer and the plane determined by the preceding monomer in the chain. For our procedure these four angles have the values: α, $\alpha + \beta$, α and $\beta - \alpha$. The average value of the torsion angle θ between the plane of one monomer and the plane of the adjacent monomer can be estimated as $(\alpha + \beta)/2$. Two cases, for which we have obtained good

* A list of fractional atomic coordinates has been deposited with the IUCr (Reference: SE0143). Copies may be obtained through The Managing Editor, International Union of Crystallography, 5 Abbey Square, Chester CH1 2HU, England.

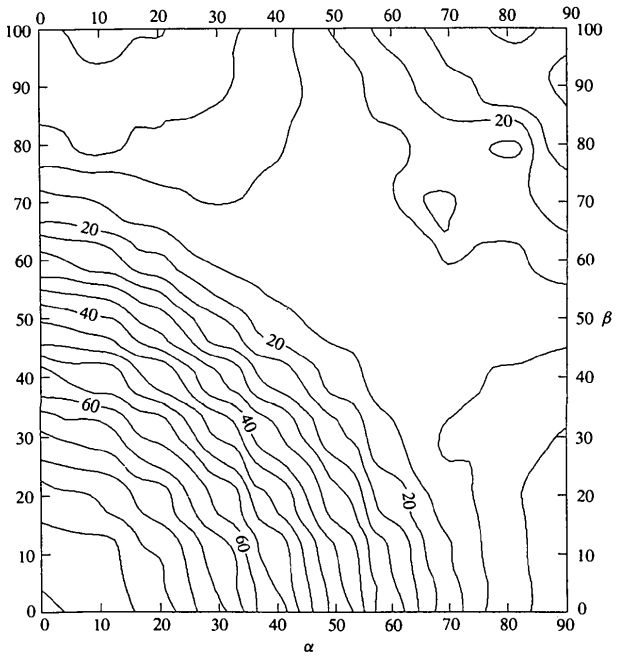

Fig. 7. Map showing the dependence of the parameter $N_{2/1}$ on the parameters α (X-axis) and β (y-axis); angles in °, $N_{2/1}$ in %.

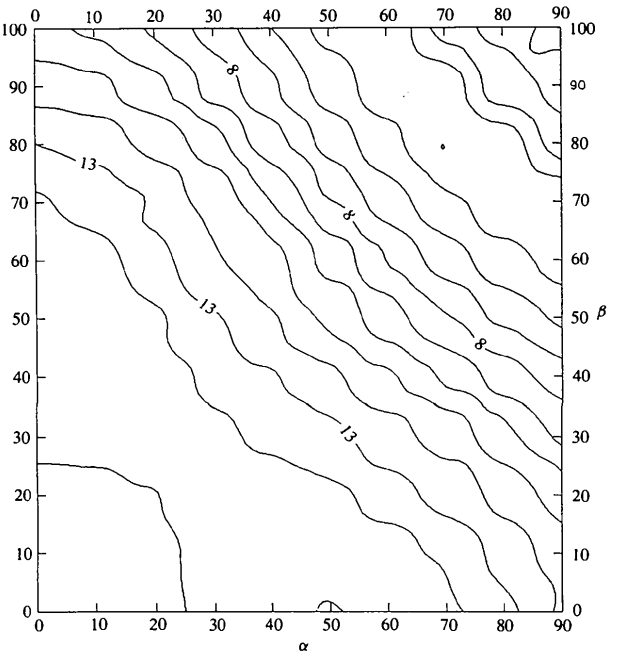

Fig. 8. Map showing the dependence of $N_{3/1}$ on α and β (notation as in Fig. 7).

Table 2. *Explanation of experimental diffraction peaks (C = crystalline, A = amorphous)*

No	Position	Origin	Indexation
1	3.7	C	100
2	6.2–7.5	C	110,200
3	9.0	C	210
4	11.1–11.9	C	300,020, 120,310
5	19.9	A	–
6	22.5–25.5	C	*ca* 20 peaks
7	25.4	A	–

correlation between the experimental and model values of N, are characterized by the same value of the mean torsion angle θ, which approximately equals 47.5°.

By comparison of the computed diffractogram, shown in Fig. 10, with the experimental one (presented in Fig. 3), it is possible to propose the final interpretation of experimental diffraction peaks. The characteristics of each peak are collected in Table 2. Comparison of the content of Table 2 with the content of Table 1 shows that in the case of this polymer it is impossible to distinguish between the peaks of crystalline origin and those of amorphous origin. Indeed, the width of a peak is not a real parameter in this case. Sometimes a peak, being the sum of few very broad Bragg reflections, is broader than the peak of amorphous origin. Of course, it is impossible to resolve such a complex peak without computer modelling.

It should be underlined, that the amorphous component of the scattered intensity can be used to obtain information about the short-range order of macromolecules in the polymer system. Such work has been carried out for PDT and its results have confirmed our model of the polymer structure (Łużny, Nizioł & Zagórska, 1994).

The poor resolution of the experimental diffraction pattern will support more than one model for the unit cell. Indeed, sometimes a triclinic unit cell is proposed (Gustaffson *et al.*, 1991). However, this paper suggests

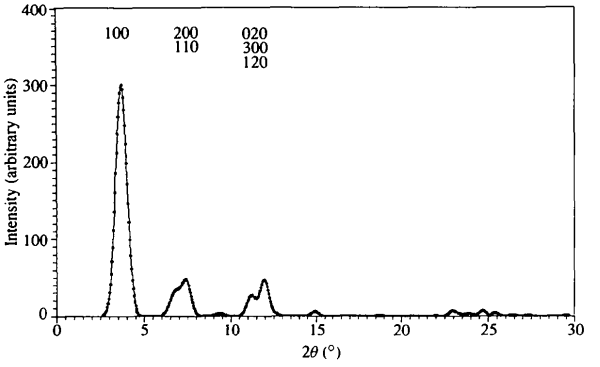

Fig. 10. Computed diffraction pattern for two model structures described by two sets of parameters: $\alpha = 30$ and $\beta = 65°$, or $\alpha = 65$ and $\beta = 30°$.

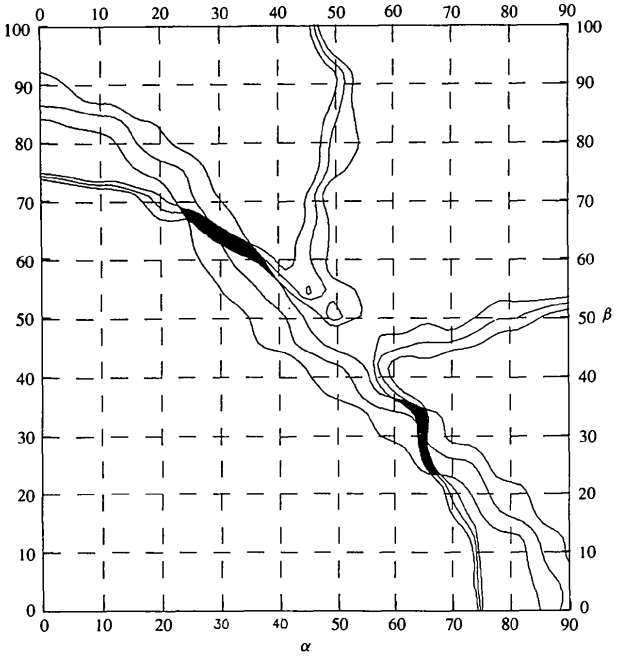

Fig. 9. Localization of regions, for which $N_{2/1}$ and $N_{3/1}$ are close to their experimental values (notation as in Fig. 7).

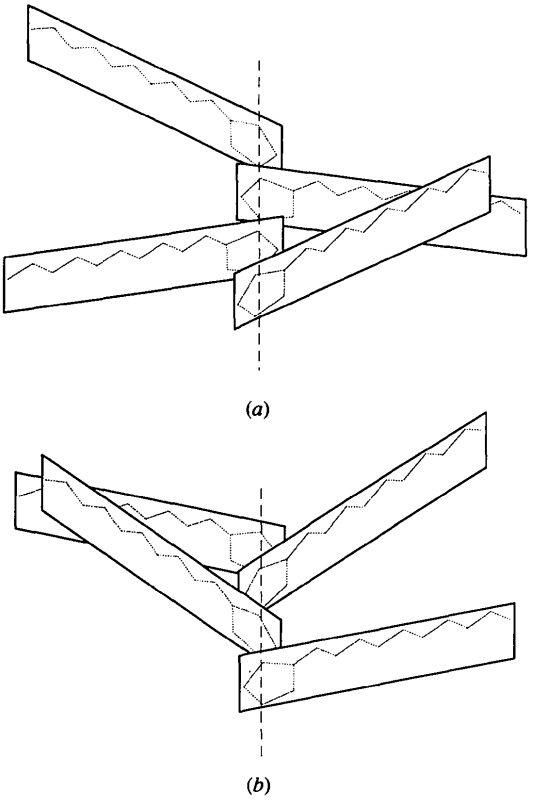

Fig. 11. Two structures with the best conformation of the PDT chain derived from the modelling described in the text.

only a hypothetical model of the structure and conformation, using the most simple arrangement of chains as a starting point, and this model can explain the real structure quite well.

One should realize that the results presented are limited by restrictions imposed on the model. For example, it is obvious that the arrangement of the side chains also has an impact on the diffraction pattern. However, this paper concentrates on the conformational defects suggested by Salaneck *et al.* (1988) and Salaneck (1989) and the influence of the conformation of the side chains on the diffraction pattern will be the subject of future work.

To summarize: we have tried to explain the influence of the conformational defects of the polymer on its diffraction pattern. This effect is very remarkable and it allows useful information on the conformation of the real polymer system to be obtained from the diffraction data. In the case of PDT, we have been able to obtain the mean torsion angle between the adjacent thiophene rings: θ is in the range 45–50°. This is important information, because the θ angle is directly related to the conjugation length, which is of significance for the value of the band gap and therefore for electronic transport properties of the polymer (Salaneck, 1989).

We realize that in the 'real' polymer the torsion angle θ has a random distribution in a wide range and it is optimistic to expect the long-range order along the main polymer chain with the unit cell containing only four monomers.

We plan to perform studies on the temperature dependence of diffraction data for PDT in order to check the correlation between the band gap, the torsion angle and the conjugation length, all *versus* temperature. This problem is connected with an effect of thermochromism, observed in poly(alkylthiophenes) (Salaneck, 1989).

The fruitful discussions with Professors S. Nizoł and A. Proń are greatly acknowledged. This work was financially supported by KBN Grants No. 300529101/p1, p2 and p3.

References

GUSTAFFSON, G., INGANÄS, O., ÖSTERHOLM, H. & LAAKSO, J. (1991). *Polymer*, **32**, 1574–1582.

ŁUŻNY, W., NIZIOŁ, S. & PROŃ, A. (1995). *J. Polym. Sci. Polym. Phys. Ed.* Submitted.

ŁUŻNY, W., NIZIOŁ, S., STRACZYŃSKI, G. & PROŃ, A. (1994). *Synth. Met.* **62**, 273–277.

ŁUŻNY, W., NIZIOŁ, S. & ZAGÓRSKA, M. (1994). *Synth. Met.* **64**, 59–62.

ŁUŻNY, W., NIZIOŁ, S., ZAGÓRSKA, M. & PROŃ, A. (1993). *Synth. Met.* **55–57**, 359–364.

ŁUŻNY, W., ŚLUSARCZYK, C. & WŁOCHOWICZ, A. (1991). Unpublished results.

MÅRDALEN, J., SAMUELSEN, E. J., GAUTUN, O. R. & CARLSEN, P. H. (1992). *Synth. Met.* **48**, 363–373.

SALANECK, W. R. (1989). *Contemp. Phys.* **30**, 403–425.

SALANECK, W. R., INGANÄS, O., THÉMANS, B., NILSSON, J. O., SJÖGREN, B., ÖSTERHOLM, J. E., BRÈDAS, J. L. & SVENSSON, S. (1988). *J. Chem. Phys.* **89**, 4613–4625.

TASHIRO, K., MINAGAWA, Y., KOBAYASHI, M., MORITA, S. & YOSHINO, K. (1993). *Synth. Met.* **55–57**, 321–326.

VISSER, G. J., HEERES, G. J., WOLTERS, J. & VOS, A. (1968). *Acta Cryst.* B**24**, 467–475.

HSU, W.-P., LEVON, K., HO, K.-S., MYERSON, A. S. & KWEI, T. K. (1993). *Macromolecules*, **26**, 1318–1327.

WINOKUR, M. J., WAMSLEY, P., MOULTON, J., SMITH, P. & HEEGER, A. J. (1991). *Macromolecules*, **24**, 3812–3821.